



## Photokilling Squamous Carcinoma Cells SCCVII with Ultrafine Particles of Selected Metal Oxides

SINIŠA IVANKOVIĆ, MARIJAN GOTIĆ,\* MISLAV JURIN AND SVETOZAR MUSIĆ

*Ruđer Bošković Institute, P.O. Box 180, HR-10002 Zagreb, Croatia*

gotic@rudjer.irb.hr

*Received February 1, 2002; Accepted July 16, 2002*

**Abstract.** The ability of ultrafine particles of  $\text{TiO}_2$ ,  $\text{WO}_3$  and iron-doped  $\text{TiO}_2$  to kill cancer cells in the presence of UV irradiation was investigated. The best photokilling effect on carcinoma cells SCCVII cultured in vitro showed iron-doped  $\text{TiO}_2$  ultrafine particles synthesized by the sol-gel procedure with starting chemicals Ti(IV)-isopropoxide and anhydrous Fe(II)-acetate. It was found that a small particle size and high dispersity influenced cytotoxicity and photocatalytic efficiency. The remarkable photokilling effect of highly iron-doped  $\text{TiO}_2$  ultrafine particles (the molar ratio  $\text{Fe}/\text{Ti} = 0.136$ ) in the presence of UV irradiation was observed. The influence of ultrafine metal oxide particles on the inhibition of cancer cell proliferation was measured using a  $^3\text{H}$ -thymidine incorporation test. The possible mechanism involved in the photokilling of carcinoma cells with ultrafine particles of selected metal oxides was discussed.

**Keywords:**  $\text{TiO}_2$ ,  $\text{WO}_3$ , iron-doped  $\text{TiO}_2$ , ultrafine particles, cancer cells, photokilling effect

### 1. Introduction

Photoexcited semiconductor metal oxide particles can be considered as small electrochemical cells able to provoke various redox reactions.  $\text{TiO}_2$  is one of the most promising photocatalysts, stable in various solvents under photoirradiation and an inexpensive material relatively easy to synthesize in the laboratory.  $\text{TiO}_2$  was extensively used as a photocatalyst in the investigation of the conversion of solar energy into chemical energy and in the environmental applications of the photooxidation of organic pollutants in drinking and waste waters [1, 2]. On the other hand, there are rather few investigations about the applications of  $\text{TiO}_2$  in biology. In early applications of  $\text{TiO}_2$  in biology Matsunaga et al. [3] showed that microbial cells in water could be killed by contact with a platinum-loaded titanium oxide powders ( $\text{TiO}_2/\text{Pt}$ ) upon illumination

with a near-UV light for 60 to 120 min. Cai et al. [4] were the first to show that HeLa cells cultured in vitro could be effectively killed in the presence of  $\text{TiO}_2$  with UV irradiation using a 500 watt mercury lamp.

Huang et al. [5] investigated the photokilling of U937 cells with ultrafine  $\text{TiO}_2$  particles produced using the sol-gel method [6, 7]. However, the photocatalytic studies with cancer cells were mainly performed with P 25  $\text{TiO}_2$ , commercially available from Degussa or Nippon-Aerosil Co. Degussa P 25  $\text{TiO}_2$  is a non-porous 75:25 anatase-to-rutile mixture with a BET surface area of about  $55 \text{ m}^2 \text{ g}^{-1}$  and crystallite sizes of  $\sim 30 \text{ nm}$  in 200 to 400 nm aggregates. The main disadvantage in practical photochemical applications of pure  $\text{TiO}_2$  phase is its relatively low absorption in the visible portion of the solar spectrum. The iron doping extended the absorption threshold of  $\text{TiO}_2$  particles into the visible part of the spectrum, whereas the substitutional doping of  $\text{TiO}_2$  particles with iron increased

\*To whom all correspondence should be addressed.

the charge-carrier lifetime from nanoseconds for pure TiO<sub>2</sub> to minutes and even hours for iron-doped TiO<sub>2</sub>. Wang et al. [8] showed a strong influence of the synthesis procedure on the distribution of iron in the TiO<sub>2</sub> matrix. The samples with a more uniform iron distribution in TiO<sub>2</sub> showed an enhanced photocatalytic activity.

In the present work we have focused on the photokilling of squamous carcinoma cells SCCVII with ultrafine particles of TiO<sub>2</sub>, WO<sub>3</sub> and iron-doped TiO<sub>2</sub>. The ability of TiO<sub>2</sub> to kill cancer cells in the presence of UV irradiation was studied by comparing the photokilling effect of the commercially available Degussa P 25 TiO<sub>2</sub> and a series of TiO<sub>2</sub> and iron-doped TiO<sub>2</sub> ultrafine particles synthesized by the sol-gel procedure in laboratory. In addition to it, the inhibition of cancer cell proliferation using the <sup>3</sup>H thymidine test was investigated.

## 2. Experimental

The experimental conditions of the synthesis of metal oxide particles are given in Table 1, whereas Table 2 shows phase composition, crystallite sizes and specific surface areas of the same metal oxide particles used in this work. Detail structural properties of iron-doped TiO<sub>2</sub> samples will be discussed elsewhere [10].

Before being added into a plastic Petri dish (manufactured by Corning) containing cultured cancer cells, the metal oxide particles (0.05 g) were ultrasonically dispersed between 3 and 8 min in water (15 ml), previously treated with Millipore-Milli-Q filtration system. The metal oxide particles were then left to sediment for 10 to 20 min, whereas the P 25 TiO<sub>2</sub> particles were centrifuged at 8000 r.p.m. for 1 min in order to separate ultrafine metal oxide particles from the particle aggregates. Thus prepared highly dispersed

Table 1. Experimental conditions for the synthesis of TiO<sub>2</sub>, iron-doped TiO<sub>2</sub> and WO<sub>3</sub> particles. History of the metal oxide particles and their properties.

Sample	Sample history
P 25	TiO <sub>2</sub> supplied by Degussa.
T94	TiO <sub>2</sub> obtained by the sol-gel procedure using 5 ml of isopropanol, 25 ml of Ti(IV)-isopropoxide, 300 ml of Re H <sub>2</sub> O and 1 ml of the HNO <sub>3</sub> catalyst is added. Synthesis performed in an oil bath at 80°C with reflux in a specially designed all-glass assembly. Sample dried in a Petri dish at 50°C for 42 h [9].
PG0	TiO <sub>2</sub> obtained by the sol-gel procedure using 75 ml of isopropanol, 25 ml of Ti(IV)-isopropoxide, 120 ml of Re H <sub>2</sub> O and 5 g of poly(ethylene) glycol (PEG). Synthesis performed in an oil bath at 70°C in a specially designed all-glass assembly with reflux and a bubbling N <sub>2</sub> . Sample dried in a Petri dish at 50°C for 48 h. Calcination performed at 500°C [10].
FT1	Iron-doped TiO <sub>2</sub> sample obtained by the sol-gel procedure using 75 ml of isopropanol, 25 ml of Ti(IV)-isopropoxide, 62 ml of Re H <sub>2</sub> O + 8 ml of 0.1 mol dm <sup>-3</sup> of Fe(NO <sub>3</sub> ) <sub>3</sub> and 50 ml of NH <sub>3</sub> (25%). The molar ratio of Fe/Ti is 0.007 as determined by PIXE <sup>a</sup> . Synthesis performed in an oil bath at 70°C in a specially designed all-glass assembly with reflux and a bubbling N <sub>2</sub> . Sample dried in a Petri dish at 50°C for 48 h. Calcination performed at 500°C [10].
NTF1	Iron-doped TiO <sub>2</sub> sample obtained by the novel sol-gel procedure using 50 ml of extra dry ethyl alcohol (99.9%), 25 ml of Ti(IV)-isopropoxide and 25 ml of a purified glacial acetic acid +0.189 g of anhydrous Fe(II)-acetate. H <sub>2</sub> O molecules for hydrolysis generated "in situ" by an esterification reaction between the acetic acid and ethanol. Synthesis is performed in an oil bath at 70°C in a specially designed all-glass assembly with reflux and a bubbling extra dry N <sub>2</sub> . Sample dried in a Petri dish at 60°C for 42 h. Calcination performed at 500°C. The molar ratio of Fe/Ti is 0.012 as determined by AAS <sup>b</sup> [10].
NTF5	Iron-doped TiO <sub>2</sub> sample obtained by the novel sol-gel procedure using 50 ml of extra dry ethyl alcohol (99.9%), 25 ml of Ti(IV)-isopropoxide and 25 ml of a purified glacial acetic acid +0.783 g of anhydrous Fe(II)-acetate. H <sub>2</sub> O molecules for hydrolysis generated "in situ" by an esterification reaction between the acetic acid and ethanol. Synthesis is performed in oil bath at 70°C in a special designed all-glass assembly with reflux and a bubbling extra dry N <sub>2</sub> . Sample dried in a Petri dish at 60°C for 66 h. Calcination performed at 580°C. The molar ratio of Fe/Ti is 0.053 as determined by AAS <sup>b</sup> [10].
NTF15	Iron-doped TiO <sub>2</sub> sample obtained by the novel sol-gel procedure using 50 ml of extra dry ethyl alcohol (99.9%), 25 ml of Ti(IV)-isopropoxide and 25 ml of a purified glacial acetic acid +2.313 g of anhydrous Fe(II)-acetate. H <sub>2</sub> O molecules for hydrolysis generated "in situ" by an esterification reaction between the acetic acid and ethanol. Synthesis performed in an oil bath at 70°C in a specially designed all-glass assembly with reflux and a bubbling extra dry N <sub>2</sub> . Sample dried in a Petri dish at 60°C for 40 h. Calcination performed at 420°C. The molar ratio of Fe/Ti is 0.136 as determined by AAS <sup>b</sup> [10].
WO <sub>3</sub>	Sample obtained by passing the 0.1 M Na <sub>2</sub> WO <sub>4</sub> solution through Dowex cation exchange resin until the pH reaches 1.8. Thus obtained clear solution was left in a closed flask at room temperature for 40 h. An intense green-yellow precipitate was formed. It was isolated by decantation and centrifugation, washed twice with doubly distilled H <sub>2</sub> O, and then dried in a Petri dish at 60°C for 48 h [11].

<sup>a</sup>The amount of iron in a sample was determined using the Proton Induced X-ray Emission (PIXE) facility at the Ruđer Bošković Institute.

<sup>b</sup>The amount of iron in a sample was determined using the Atomic Absorption Spectroscopy (AAS).

Table 2. Phase composition, crystallite sizes and specific surface areas of the metal oxide particles used in this work.

Sample	XRD phase composition (approximate molar fraction) <sup>a,b</sup>	Raman phase composition	Crystallite size <sup>b</sup> /nm	Specific surface area by B.E.T./m <sup>2</sup> g <sup>-1</sup>
P 25	Anatase + Rutile (0.3)		30	78.5 <sup>c</sup>
T94	Anatase + Brookite (small amount)	Anatase <sup>d</sup> (dominant phase) + Brookite	7.8	
PG0	Anatase + Brookite (small amount)		15	
FT1	Anatase	Anatase	30	
NTF1	Anatase + Rutile (0.05)	Anatase	17	43.8
NTF5	Rutile + Anatase (0.5)	Anatase + Rutile (~50 mol%)	19	24.1
NTF15	Anatase + Rutile (0.03) + very small amount of unidentified phase		9	102.3
WO <sub>3</sub>	WO <sub>3</sub> • H <sub>2</sub> O		<100	

<sup>a</sup>Approximate molar fraction determined by XRD patterns;

<sup>b</sup>Crystallite size of anatase determined by broadening the most intense anatase diffraction line;

<sup>c</sup>The specific surface area declared by manufacturer is ~55 m<sup>2</sup>g<sup>-1</sup>;

<sup>d</sup>Particle diameter determined from the position of Low-frequency Raman peak was 8.8 nm [10].

aqueous suspensions of ultrafine metal oxide particles were employed in cytotoxicity experiments. The concentration of ultrafine particles in the aqueous suspension was determined by a simple calculation of the weight/volume ratio, after the evaporation of an aqueous phase up to dryness from the known volume of an aqueous suspension.

Squamous carcinoma cells SCCVII (mice C3H strain) were cultured in a RPMI 1640 medium supplemented with 10% fetal calf serum in a humidified incubator with an atmosphere of 5% CO<sub>2</sub> in air at 37°C. Before plating the cells were counted by using the trypan blue cell viability test and the initial concentration of cells in each Petri dish was fitted to ≈10<sup>5</sup> cells ml<sup>-1</sup>.

The squamous cells were plated as a monolayer culture in 30 mm plastic Petri dishes for 24 h at 37°C in CO<sub>2</sub> to allow cell attachment. 400 μL of an aqueous metal oxide suspension was added into each Petri dish with 3 ml of medium during the exponential growth of cells (≈10<sup>5</sup> cells ml<sup>-1</sup>). The final concentrations of ultrafine metal oxide particles in Petri dishes containing cultured cells were ranged from 35 to 100 μg ml<sup>-1</sup>. It was proved that the concentration gap between 35 and 100 μg ml<sup>-1</sup> had no effect on cytotoxicity results. The cells were recultured in the presence of ultrafine metal oxide particles at 37°C for 24 h in the dark, then the old cultured medium was replaced with a freshly prepared RPMI 1640 medium. The observation of cancer cells before and after the addition of metal oxide particles by an inverted phase-contrast microscope showed that metal oxide particles were well distributed in Petri dishes and that most of them were incorporated into the cells. The morphology of the cells was not changed on addition of ultrafine metal oxide particles.

The cells thus prepared in 30 mm Petri dishes were irradiated with a home-made apparatus (metal halide lamp, 2000 W, model Philips HPI-T 2000/220 V without a hard glass tubular envelope). The quartz lens of 3" diameter having 150 mm focus length was used in order to obtain concentrated parallel light beams. The UV irradiation experiments were performed by using bandpass filters, provided by Schott, Germany, Catalog No. KG-3, thickness 2 mm, to minimize IR radiation and No. UG-1, thickness 2 mm, to obtain UV irradiation between 320 nm and 396 nm (maximum relative transmission of 55% at 365 nm). The UV light intensity at the liquid surface of a Petri dish with attached cells was 7 to 8 mW cm<sup>-2</sup>, as measured by the Pyroelectric Radiometer Rk-5100, Laser Precision Corporation. Hyperthermia effect was avoided, since the temperature of the medium measured at the position of the Petri dish during the UV experiments (30 cm from the lamp) did not exceed 37°C.

After irradiation the medium was again replaced with a freshly prepared RPMI 1640 medium. The irradiated cells and control cells with or without metal oxide particles were recultured for 24 h and the cell viability test was performed by using the standard trypan blue method.

Cytotoxicity to cancer cells was determined for the cells treated with (a) ultrafine metal oxide particles without irradiation, (b) ultrafine metal oxide particles in the presence of UV irradiation and (c) UV irradiation alone. Each cytotoxicity result was an average value of three measurements.

To check the proliferative ability of survived cancer cells after treatments a, b or c described above, a standard <sup>3</sup>H-thymidine incorporation test was

performed. For this purpose the survived cells after treatments a, b or c were trypsinated and recultured in 96 well plates for 48 h. In each well  $\sim 10^4$  cells resuspended in 200  $\mu\text{L}$  of the RPMI 1640 medium supplemented with 10% fetal calf serum were added. After that, 25  $\mu\text{L}$  of radioactive  $^3\text{H}$ -thymidine ( $6\text{-}^3\text{H}$ -thymidine, Amersham, specific radioactivity 24 Ci  $\text{mmol}^{-1}$ ) was added and the cells were recultured for the next 24 h (altogether 72 h). Cultivation was then terminated and the cell cultures were filtered using the filters (Schleicher Schuell, Dassel, Germany) with a PHD Cell Harvester (Cambridge Technology Inc., Watertown, USA). The degree of radioactivity in the cells was determined using a  $\beta$ -scintillation counter (Wallac 1209 Rockbeta Liquid Scintillation Counter Pharmacy, Uppsala, Sweden). The results of the  $^3\text{H}$ -thymidine incorporation test were expressed as a mean value ( $\pm$ standard deviation) of four replications. Statistical significance of differences between the control cells and the specific ultrafine metal oxide particles was evaluated using the unpaired two-sided student's-t-test.  $P$  levels  $<0.05$  were considered significant.

### 3. Results and Discussion

The cytotoxicity of selected metal oxide semiconductor particles to squamous carcinoma cells cultured in the dark is shown in Fig. 1. The cytotoxicity of oxide particle to the cells was investigated using two different types of aqueous suspensions. The first suspension was prepared by redispersion of as-synthesized or as-received metal oxide particles in Milli-Q water. The second suspension was obtained by collecting the finely dispersed particles from the surface of the first aqueous suspension. The open bars represent the cytotoxicity to carcinoma cells cultured in the presence of lowly dispersed aqueous suspension, whereas the dark bars represent the cytotoxicity to cells cultured in the presence of highly dispersed (ultrafine) metal oxide particles. Figure 1 indicates that the surviving fraction of the cell was on the average greater than approximately 0.7 when the well dispersed (ultrafine) metal oxide particles from the second suspension were applied. On the contrary, poorly dispersed metal oxide particles were very toxic to carcinoma cells and the surviving fraction of the cell decreased enormously. The final concentration of metal oxide particles in the medium with cultured cancer cells ranged from 35 to 100  $\mu\text{g ml}^{-1}$ . In this concentration range there was no significant influence of the concentration on the cytotoxicity of cancer

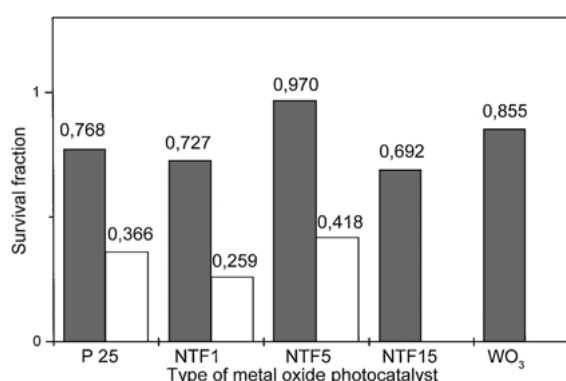


Figure 1. The survival fraction of squamous carcinoma cells cultured in the dark in the presence of various types of metal oxide particles. Open bars show the results of the survival fraction of cells cultured in the presence of lowly-dispersed metal oxide particles, whereas black bars show the results of survival fraction of cancer cells cultured in the presence of highly-dispersed metal oxide particles, i.e. most of them were incorporated into the cells (see the experimental section). The history of metal oxide samples and their notations are given in Table 1. The concentration of metal oxide particles in a medium with cultured cancer cells was in the range of 35 to 100  $\mu\text{g ml}^{-1}$ . Cancer cells cultured with no ultrafine metal oxide particles were used as a control probe. The survival fraction of 1 corresponds to the average number of cells in a control probe (1,289,000 cells per 3 ml of medium in a 30 mm plastic Petri dish). Experiments were performed in triplets and repeated three times.

cells, thus proving that a small particle size and high dispersity were important parameters in determining the cytotoxicity of metal oxide particles to cancer cells.

Figure 2 shows the results of the surviving fraction of squamous carcinoma cells in dependence on the type of metal oxide photocatalyst upon irradiation with UV light for 10 min. The UV irradiation itself showed a little cytotoxic effect on SCVII cells (surviving fraction 0.773). In the presence of UV irradiation and ultrafine metal oxide particles the cells were killed more effectively. Among the metal oxide particles investigated in the present work, the  $\text{WO}_3$  photocatalyst showed the lowest photokilling effect. Standard photocatalyst P 25  $\text{TiO}_2$  showed a better photocatalytic activity in the killing of cancer cells than  $\text{WO}_3$ , but still much less than the pure  $\text{TiO}_2$  (samples T94 and PG0) produced in the present work by the sol-gel procedure.

The iron-doped  $\text{TiO}_2$  sample, FT1 (the molar ratio of Fe/Ti is 0.007), produced by the sol-gel procedure under alkaline conditions showed an intermediate photocatalytic effect on the killing of SCVII cells, comparable with the photocatalytic activity of undoped  $\text{TiO}_2$  (samples T94 and PG0). The best photokilling effect showed the iron-doped samples NTF1, (the

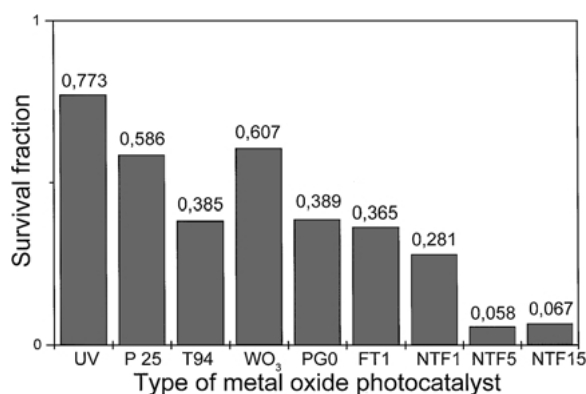


Figure 2. The survival fraction of squamous carcinoma cells upon their irradiation for 10 minutes with UV light alone (UV) and with UV light in the presence of various types of ultrafine metal oxide particles (P 25 to NTF15). In the UV irradiation experiment alone (survival fraction 0.773), the control probe was the number of cells cultured in the dark without an addition of metal oxide particles. The number of survived cells cultured in the dark with metal oxide particles was used as a control probe in the UV + cancer cells + metal oxide irradiation experiments. The notations of samples are given in Table 1.

molar ratio of Fe/Ti is 0.012), NTF5 (the molar ratio of Fe/Ti is 0.053) and NTF15 (the molar ratio of Fe/Ti is 0.136), synthesized by the sol-gel procedure using Ti(IV)-isopropoxide and anhydrous Fe(II)-acetate as precursors of titanium and iron. In this synthesis procedure the precursors were mixed and subsequently hydrolyzed with H<sub>2</sub>O molecules generated in situ by an esterification reaction between the acetic acid and alcohol. It was expected that the distribution of iron in TiO<sub>2</sub> of the particles synthesized by this sol-gel procedure would be the most uniform and, consequently, these samples showed the best photokilling effect.

After the treatment in the dark or in the presence of UV irradiation, the survived cancer cells could be easily recovered by exponential growth, in case they had not lost their ability to synthesize new DNA molecules. To check this, the <sup>3</sup>H-thymidine incorporation test was conducted. Figure 3 shows the incorporation of <sup>3</sup>H-thymidine into the survived cells after their reculturing in optimal conditions for 72 h (<sup>3</sup>H-thymidine during the last 24 h). The Control bar represents the survived cancer cells alone after their culturing in the dark. All other experiments in the dark (black bars) were performed in the presence of metal oxide particles and their values of <sup>3</sup>H-thymidine incorporation into cells were tested with respect to the Control bar using the unpaired two-sided student's-t-test. A slight decrease

in the <sup>3</sup>H-thymidine incorporation with the increase in iron doping of the NTF1, NTF5 and NTF15 samples cultured in the dark is visible, but this decrease is not statistically significant. Only the survived cells cultured in the presence of P 25 in the dark showed a significant inhibition of <sup>3</sup>H-thymidine incorporation (asterisk-marked). This could be explained by a different origin of P 25 TiO<sub>2</sub> preparation in comparison with the iron-doped samples. Commercially available P 25 TiO<sub>2</sub> photocatalyst was synthesized by aerosol techniques, whereas our samples were originally synthesized using the sol-gel technique. It is obvious that the photocatalysts obtained by the sol-gel technique are less dangerous in the term of proliferation of the survived cancer cells than the commercially available P 25 TiO<sub>2</sub> after culturing in the dark.

The effect of UV light with or without the presence of metal oxide particles on the inhibition of cell proliferation is shown by open bars in Fig 3. Each UV result was tested against its counterpart in the dark. UV irradiation alone significantly inhibited cell proliferation compared with the control in the dark. Iron-doped samples also significantly inhibited cell proliferation in comparison with their controls in the dark. Moreover, the highest inhibition of cell proliferation shows the lowest iron-doped sample (the difference between NTF1 and NTF1UV). With the increasing iron content in iron-doped TiO<sub>2</sub> samples, the incorporation of <sup>3</sup>H-thymidine into cancer cells was steadily increasing. Sample P 25 shows by far the highest inhibition of <sup>3</sup>H-thymidine incorporation. However, when comparing the <sup>3</sup>H-thymidine incorporation level of P 25 sample activated by UV irradiation with its counterpart in the dark (P25 and P25UV), the relative inhibition of <sup>3</sup>H-thymidine incorporation becomes statistically significant. This value is relatively the same as for the highest iron-doped TiO<sub>2</sub> sample NTF15. The NTF1 and NTF5 samples show a relatively much higher inhibition of <sup>3</sup>H-thymidine into cancer cells than P 25, due to high inhibition of <sup>3</sup>H-thymidine incorporation into P 25 itself in the dark.

In reference literature the photocatalytic reactions of fine particles of WO<sub>3</sub> [12], TiO<sub>2</sub> [13] and iron-doped TiO<sub>2</sub> [8, 14–18] in an aqueous medium are well documented. It can be suggested that the photocatalytic reactions also play an important role in photokilling cancer cells with ultrafine particles of selected metal oxides. This photocatalytic process generates Reactive Oxygen Species (ROS) which, in principle, may be fatal for cancer cells. It is important to note that the

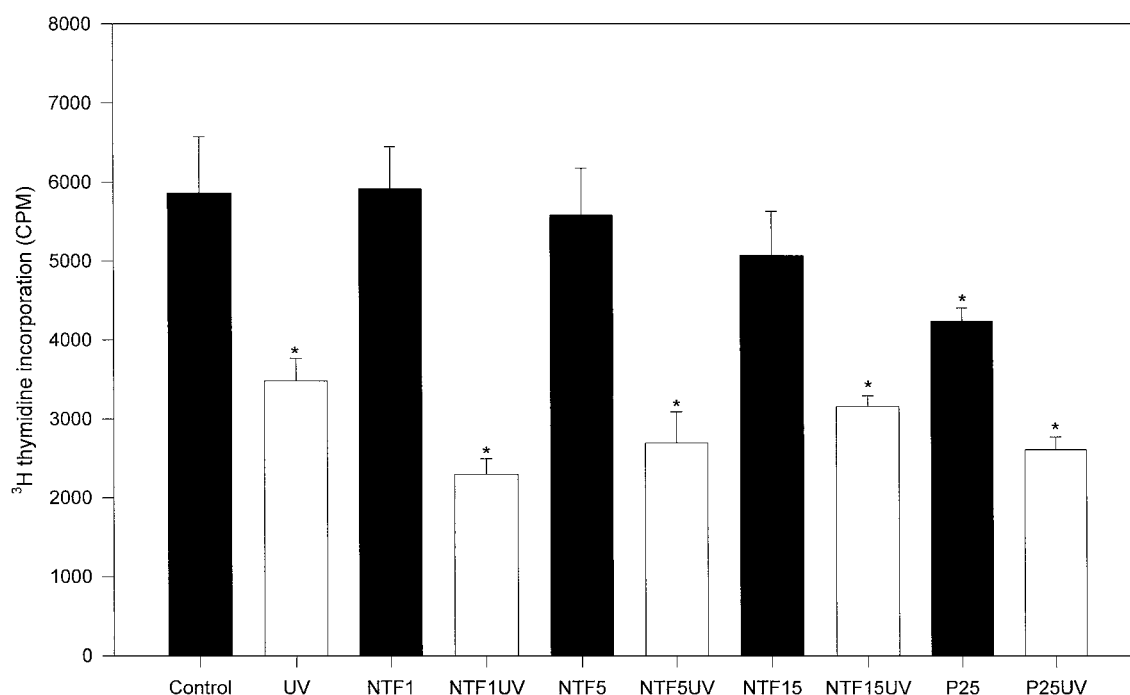
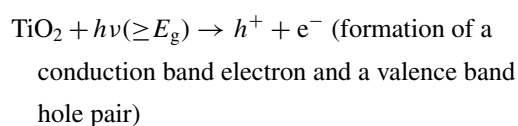


**Figure 3.** <sup>3</sup>H thymidine incorporation into SCCVII cells recultured for 72 h (<sup>3</sup>H thymidine during the last 24 h) alone (Control) or with the ultrafine metal oxide particles exposed to either UV (open bars) or culturing in the dark (black bars). The results of <sup>3</sup>H-thymidine test were expressed as mean value  $\pm$  standard deviations of four replicates. The lower amount of incorporation of <sup>3</sup>H-thymidine into the cells verifies the higher degree of inhibition of cell proliferation. CPM denotes the number of counts per minute. The measurements marked with an asterisk (\*) document a significant inhibition of cell proliferation with the accuracy greater than the 0.05 probability level. ( $P < 0.05$ ). All samples cultured in the dark were statistically tested against the control cells alone, also cultured in the dark (Control), while each measurement obtained in the UV experiments (open bars) were tested in respect of their counterparts in the dark (black bar on the left). Only the P 25 TiO<sub>2</sub> shows a significant inhibition of cancer cells proliferation after culturing in the dark, whereas in the presence of UV light all samples and UV irradiation alone (open bars) show a significant inhibition of survived cancer cells proliferation in comparison with their counterparts cultured in the dark. The relative incorporation of <sup>3</sup>H-thymidine into survived cancer cell in the presence of UV irradiation increases continuously with the increase of iron content in the iron-doped TiO<sub>2</sub> ultrafine particles (NTF15 > NTF5 > NTF1).

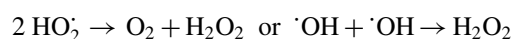
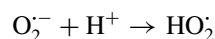
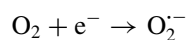
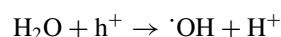
particles of selected metal oxides must be of nanometric dimensions, so that they can penetrate into the cancer cells and take over the photokilling role to these cells.

The mechanism of photokilling cancer cells using selected ultrafine metal oxide particles is of a very complex nature [3–5, 19–21]. Nevertheless, in this respect the photochemical reactions at the interface MO/water (MO = metal oxide) must be taken into account. For example, the UV irradiation of very fine TiO<sub>2</sub> particles will produce the electron/hole pairs:

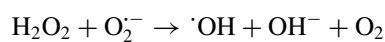


These electron/hole pairs will in an aqueous suspension of colloidal TiO<sub>2</sub> induce a series of photochemical re-

actions generating ROS, as follows:



(nonproductive radical reactions)



Generally, the improved photocatalytic performance of iron-doped TiO<sub>2</sub> could be explained by iron centers acting as shallow traps for the valence band holes, whereas electrons are trapped at Ti(IV) surface sites. Local separation of electrons at the surface of ultrafine particles and the iron centers distributed over the whole volume of the particle are responsible for the

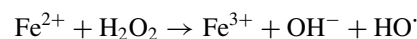
inhibition of electron/hole recombination [22]. In photocatalytic oxidation of an organic pollutant with iron-doped TiO<sub>2</sub>, the best photocatalytic activity showed a low loaded iron-doped TiO<sub>2</sub> within the solubility limit of iron in the TiO<sub>2</sub> matrix (about 1 mol% of doped iron). Heavily iron loaded TiO<sub>2</sub> samples are photocatalytically inactive due to formation of separated iron oxide phases that form heterojunctions, thus encouraging electron-hole recombination [14, 15]. However, in the present work an excellent photoactivity of relatively highly iron-doped TiO<sub>2</sub> samples under UV irradiation in the killing of SCCVII cancer cells was observed. This effect may be explained by the specific structural and microstructural properties of synthesized iron-doped TiO<sub>2</sub> ultrafine particles. In addition to this, a different role of iron ions in non-living and living environments cannot be excluded.

The attack by ROS, generated by the photocatalytic process outside the cells has been reported to be the initial mode of killing bacteria and other types of cells [20, 21]. Iron-doped TiO<sub>2</sub> ultrafine particles can be ingested into cancer cells, so there is a possibility of photocatalytic attacks inside the cells.

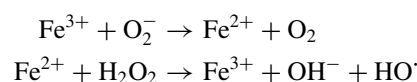
Navio et al. [15] reported the dissolution of 5 at% of iron into the TiO<sub>2</sub> matrix. The dissolution was expected to be more extensive under the UV irradiation. In a near-neutral pH medium a hole-driven photo-oxidation of surface >Fe-OH sites to (>Fe-OH)<sup>+</sup> sites is reported [23], whereas at higher pH values the reductive dissolution of Fe<sup>3+</sup> ions is present. The photoreduction of Fe<sup>3+</sup> ions by dissolved organic substances in seawater was also reported [24], and, based on that investigation, it was suggested that organic matter was responsible for the photoreduction of Fe<sup>3+</sup> ions in seawater. Since in the present case very fine iron-doped TiO<sub>2</sub> particles are incorporated into carcinoma cells, there is a real possibility of the reduction of Fe<sup>3+</sup> to Fe<sup>2+</sup> upon UV and visible light irradiation. Moreover, the process of phagocytosis allowed the cells to uptake a relatively very large amount of iron in the form of iron-doped TiO<sub>2</sub> ultrafine particles. The iron incorporated into the cells can be dissolved and in accordance with the photochemistry of Fe<sup>2+</sup> in an aqueous medium, the reactive oxygen species (ROS) can be produced by the photolysis of surface or homogeneous complexes via the Fenton-type photo reaction [15, 20].

Upon the UV irradiation in the presence of a photocatalyst, along with highly reactive hydroxyl radicals and superoxide ions, hydrogen peroxide can be

produced. H<sub>2</sub>O<sub>2</sub> can be activated by a ferrous ion via the Fenton reaction, in which H<sub>2</sub>O<sub>2</sub> decomposes into a hydroxyl radical and a hydroxide anion through the reductive cleavage with a ferrous ion [20]:



The HO<sup>•</sup> formed is very reactive and able to continue interacting with the iron species, thus generating additional hydroxyl radicals via the Fenton reaction. When both H<sub>2</sub>O<sub>2</sub> and the superoxide ion are present, catalytic amounts of the ferric ion may participate in the iron catalysed Haber-Weiss reaction [20] to yield more hydroxyl radicals, as follows,



thus increasing the photokilling effect of TiO<sub>2</sub> on carcinoma cells.

The present investigation showed dependence of cancer cells proliferation on the content of iron fraction in iron-doped TiO<sub>2</sub> ultrafine particles. From reference literature it is known that iron participates in a range of reactions that are necessary for cell viability and cell proliferation. For example, Furukawa et al. [25] showed that exposure of cells to anti-transferrin receptor antibody, which blocked the iron supplement into the cells, caused a decrease in ribonucleotide reductase activity and DNA synthesis. Decrease in DNA synthesis was restored by the addition of iron in the form of ferric nitriloacetate. These results showed that the iron-supply regulated cell proliferation. Laskey et al. [26] showed that the inhibited proliferation of both Raji and murine erythroleukemia cells were rescued upon the addition of ferric salicylaldehyde isonicotinoyl hydrazone (Fe-SIH), due to delivery of iron to Raji cells in the presence of the blocking anti-transferrin receptor antibodies. In addition, it was found that Fe-SIH slightly stimulated DNA synthesis in phytohemagglutinin-stimulated peripheral blood lymphocytes. Chenoufi et al. [27] showed that DNA synthesis was likely to be related both to cell proliferation and to DNA repair. Zager et al. [28] showed that Oxypurinol and ·OH scavengers (benzoate; dimethylthiourea) suppressed in vitro tubular cell proliferation, while "catalytic" iron (FeSO<sub>4</sub>) had a growth-stimulatory effect. Chan et al. [29] showed that the variant Chinese hamster ovary (CHO) cells, which

were unable to acquire transferrin iron via the receptor pathway, were able to uptake iron independently from inorganic iron salts and thus provided cells with a sufficient amount of iron for DNA synthesis and cell proliferation.

In the present work a continuous increase in  $^3\text{H}$ -thymidine incorporation into cancer cells with the increased iron doping in iron-doped  $\text{TiO}_2$  samples was observed (Fig. 3). It can be concluded that iron assisted in the recovery of cancer cells after the UV treatment. This tendency could be attributed to photochemically activated iron that provided cells with a sufficient amount of iron to stimulate the synthesis of new DNA molecules and had a growth-stimulatory effect on the survived cancer cells after UV treatment. Therefore, our measurements showed two different roles of iron in the processes investigated. In the first case, the presence of iron dopant in ultrafine  $\text{TiO}_2$  particles stimulated the photokilling of cancer cells under UV irradiation. In the second case, when the cancer cells were recultured for 72 h in the dark after UV irradiation, iron provided the recovery of cell proliferation.

#### 4. Conclusions

The present work indicates that squamous carcinoma cells SCCVII cultured in vitro can be killed by ultrafine particles of  $\text{TiO}_2$ ,  $\text{WO}_3$  and iron-doped  $\text{TiO}_2$  combined with UV irradiation. The best photocatalytic performance in killing the SCCVII cells was observed for iron-doped  $\text{TiO}_2$  ultrafine particles irradiated with UV light. The enhanced photocatalytic activity of iron-doped  $\text{TiO}_2$  ultrafine particles in killing cancer cells in the presence of UV irradiation may arise from the dissolution of iron, thus generating additional hydroxyl radicals by means of the photo Fenton and iron catalyzed Haber-Weiss reactions. It was shown that one of the key parameters of the cytotoxicity of cancer cells and a good photocatalytic efficiency of metal oxide photocatalyst is the degree of dispersion of ultrafine metal oxide particles. In the UV irradiation experiments, the inhibition of  $^3\text{H}$ -thymidine incorporation into the survived cancer cells continuously decreased with the increase in iron content in the iron-doped  $\text{TiO}_2$  ultrafine particles. The iron dopant in ultrafine  $\text{TiO}_2$  particles showed two different behaviors; (a) iron stimulated the photokilling of cancer cells under UV irradiation and (b) iron provided the recovery of cells proliferation after reculturing in the dark.

#### Acknowledgments

The authors wish to thank Ms Nataša Šijaković, for synthesizing some of the iron-doped metal oxide particles used in this study, dr. Hrvoje Zorc for measurements of UV light intensities and Ms Nevenka Hiršl for assistance in biological experiments. The financial support from the Ministry of Science and Technology (research project P0903) is greatly appreciated.

#### References

1. D.A. Tryk, A. Fujishima, and K. Honda, *Electrochim. Acta* **45**, 2363 (2000).
2. M.A. Malati, *Environ. Technol.* **16**, 1093 (1995).
3. T. Matsunaga, R. Tomoda, T. Nakajima, and H. Wake, *FEMS Microbiol. Lett.* **29**, 211 (1985).
4. R. Cai, Y. Kubota, T. Shuin, H. Sakai, K. Hashimoto, and A. Fujishima, *Cancer Res.* **52**, 2346 (1992).
5. Ning-ping Huang, Min-hua Xu, Chun-wei Yuan, and Rui-rong Yu, *J. Photochem. Photobiol. A: Chem.* **108**, 229 (1997).
6. C. Kormann, D.W. Bahnemann, and M.R. Hoffmann, *J. Phys. Chem.* **92**, 5196 (1988).
7. B. O'Regan, J. Moser, M. Ardeson, and M. Grätzel, *J. Phys. Chem.* **94**, 8720 (1990).
8. C.-Y. Wang, D.W. Bahnemann, and J.K. Dohrmann, *Chem. Commun.* 1539 (2000).
9. S. Musić, M. Gotić, M. Ivanda, S. Popović, A. Turković, R. Trojko, A. Sekulić, and K. Furić, *Mater. Sci. Engin.* **B47**, 33 (1997).
10. N. Šijaković-Vujičić, M. Gotić, S. Musić, M. Ivanda, and S. Popović, submitted for publication in *J. Sol-Gel Sci. Technol.*
11. M. Gotić, M. Ivanda, S. Popović, and S. Musić, *Mater. Sci. Engin.* **B77**, 193 (2000).
12. G.R. Bamwenda, K. Sayama, and H. Arakawa, *J. Photochem. Photobiol. A: Chem.* **122**, 175 (1999).
13. A. Hagfeldt and M. Grätzel, *Chem. Rev.* **95**, 49 (1995).
14. M.I. Litter and J.A. Navío, *J. Photochem. Photobiol. A: Chem.* **84**, 183 (1994).
15. J.A. Navío, G. Colón, M.I. Litter, and G.N. Bianco, *J. Mol. Catal. A: Chemical* **106**, 267 (1996).
16. K.T. Ranjit and B. Viswanathan, *J. Photochem. Photobiol. A: Chem.* **108**, 79 (1997).
17. N.J. Peill, L. Bourne, and M.R. Hoffmann, *J. Photochem. Photobiol. A: Chemical* **108**, 221 (1997).
18. B. Pal, M. Sharon, and G. Nogami, *Mater. Chem. Phys.* **59**, 254 (1999).
19. H. Sakai, E. Ito, R.-X. Cai, T. Yoshioka, Y. Kubota, K. Hashimoto, and A. Fujishima, *Biochim. Biophys. Acta* **1201**, 259 (1994).
20. D.M. Blake, P.-C. Maness, Z. Huang, E.J. Wolfrum, W.A. Jacoby, and J. Huang, *Sep. Purif. Methods* **28**, 1 (1999).
21. P.-C. Maness, S. Smolinski, D.M. Blake, Z. Huang, E.J. Wolfrum, and W.A. Jacoby, *Appl. Environ. Microbiol.* **65**, 4094 (1999).
22. J. Moser, M. Grätzel, and R. Gallay, *Helv. Chim. Acta* **70**, 1596 (1987).



23. Z. Zhang, C. Boxall, and G. H. Kelsall, *Coll. Surfaces A: Physicochemical and Engineering Aspects* **73**, 145 (1993).
24. K. Kuma, S. Nakabayashi, Y. Suzuki, Isao Kudo, and K. Matsunaga, *Marine Chem.* **37**, 15 (1992).
25. T. Furukawa, Y. Naitoh, H. Kohno, R. Tokunaga, and S. Taketani, *Life Sciences* **50**, 2059 (1992).
26. J. Laskey, I. Webb, H.M. Schulman, and P. Ponka, *Experimental Cell Research* **176**, 87 (1988).
27. N. Chenoufi, O. Loreal, B. Drenou, S. Cariou, N. Hubert, P. Leroyer, P. Brissot, and G. Lescoat, *Journal of Hepatology* **26**, 650 (1997).
28. R.A. Zager, S.M. Fuerstenberg, P.H. Baehr, D. Myerson, and B. Torok-Storb, *J. Am. Soc. Nephrol.* **4**, 1588 (1994).
29. R.Y. Chan, P. Ponka, and H.M. Schulman, *Experimen. Cell Res.* **202**, 326 (1992).